BIOCHEMISTRY
including biophysical chemistry & molecular biology

Article

pubs.acs.org/biochemistry

Specific Fluorine Labeling of the HyHEL10 Antibody Affects Antigen Binding and Dynamics

Mauro Acchione,[†,⊥] Yi-Chien Lee,[‡,@] Morgan E. DeSantis,[†,#] Claudia A. Lipschultz,[†] Alexander Wlodawer,[§] Mi Li,[§,∥] Aranganathan Shanmuganathan,[†,▽] Richard L. Walter,[†,●] Sandra Smith-Gill,*[,†] and Joseph J. Barchi, Jr.*[,‡]

[†]Structural Biophysics Laboratory, Center for Cancer Research, Frederick National Laboratory for Cancer Research, Frederick, Maryland 21702, United States

[‡]Chemical Biology Laboratory, Center for Cancer Research, Frederick National Laboratory for Cancer Research, Frederick, Maryland 21702, United States

[§]Macromolecular Crystallography Laboratory, Center for Cancer Research, Frederick National Laboratory for Cancer Research, Frederick, Maryland 21702, United States

[∥]Basic Research Program, SAIC-Frederick, Frederick, Maryland 21702, United States

Supporting Information

ABSTRACT: To more fully understand the molecular mechanisms responsible for variations in binding affinity with antibody maturation, we explored the use of site specific fluorine labeling and ^{19}F nuclear magnetic resonance (NMR). Several single-chain (scFv) antibodies, derived from an affinity-matured series of anti-hen egg white lysozyme (HEL) mouse IgG1, were constructed with either complete or individual replacement of tryptophan residues with 5-fluorotryptophan (^{5F}W). An array of biophysical techniques was used to gain insight into the impact of fluorine substitution on the overall protein structure and antigen binding. SPR measurements indicated that ^{5F}W incorporation lowered binding affinity for the HEL antigen. The degree of analogue impact was residue-dependent, and the greatest decrease in affinity was observed when ^{5F}W was substituted for residues near the binding interface. In contrast, corresponding crystal structures in complex with HEL were essentially indistinguishable from the unsubstituted antibody. ^{19}F NMR analysis showed severe overlap of signals in the free fluorinated protein that was resolved upon binding to antigen, suggesting very distinct chemical environments for each ^{5F}W in the complex. Preliminary relaxation analysis suggested the presence of chemical exchange in the antibody−antigen complex that could not be observed by X-ray crystallography. These data demonstrate that fluorine NMR can be an extremely useful tool for discerning structural changes in scFv antibody−antigen complexes with altered function that may not be discernible by other biophysical techniques.

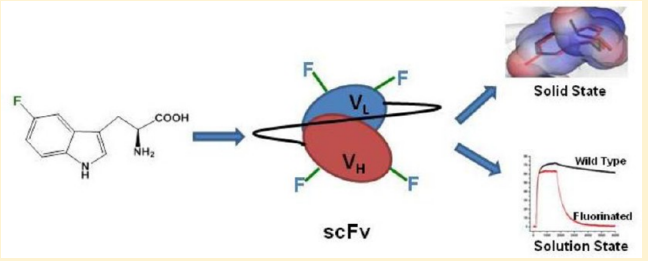

Antibodies are of considerable interest to structural biologists as extremely useful, naturally occurring models for designing and studying specific, tight-binding protein−protein interactions. Immunoglobulins share a very similar structural fold that provides a stable platform for supporting remarkable sequence plasticity while retaining function (e.g., immune surveillance and foreign molecule recognition). X-ray crystallographic structures of numerous antibody−antigen complexes are available,[1−4] and much has been learned about the importance of shape complementarity, hydrogen bonding, salt bridge formation, solvent interactions, and the hydrophobic environment at the binding interface. However, structures of uncomplexed antibodies are comparatively rare.[5] The free antibody is expected to be much more flexible, particularly in the complementarity-determining region (CDR) loops; this conformational heterogeneity is likely a major contributing factor in the difficulty in obtaining crystals suitable for diffraction. In those studies in which both the free and complexed immunoglobulin structures are available, it is clear that the static representations afforded by crystallography alone often do not fully explain differences in specificity or binding affinity that are observed.[6] This is of particular importance when attempting (1) to understand adaptation and eluding of host defenses by certain pathogens or (2) to develop antibody therapeutics with increased efficacy. There is a clear need for methods that can provide novel detailed site specific information about structure, chemical environment, and flexibility that can supplement and support X-ray crystallography data and provide new insights into altered function introduced by mutations.

Received: April 10, 2012
Revised: June 22, 2012
Published: July 6, 2012

   dx.doi.org/10.1021/bi300455t | *Biochemistry* 2012, 51, 6017−6027

Besides in silico experiments using molecular dynamics simulations, there are very few methods currently available for measuring flexibility in proteins. Kinetics and thermodynamics can provide solution state indirect evidence for dynamics on the macro level. Arguably, nuclear magnetic resonance (NMR) is the only technique that offers structural, chemical, and dynamic information at the atomic level under biologically relevant (and adaptable) solution conditions.[7−9]

Recently, ^{19}F NMR has advanced considerably as a tool for the investigation of biological molecules,[10] particularly in the solid state for membrane proteins.[11] Replacement of naturally occurring amino acids (e.g., phenylalanine and tryptophan) with a modified amino acid that can act as a ^{19}F NMR active probe offers the potential to provide a specific and sensitive measure of changes in environment and flexibility in solution before and after the binding event. Combined with high-resolution structural data, kinetics, and thermodynamic measurements, this information can be used in the engineering of proteins with very high affinity and specific recognition by directing decisions on specific mutations. As an NMR probe, ^{19}F has distinct advantages in biological investigations. The ^{19}F isotope is 100% naturally abundant, making it second only to ^{1}H in NMR sensitivity. Unlike commonly used NMR probes such as ^{13}C and ^{15}N, ^{19}F-labeled molecules do not suffer from high biological background. Together, these two attributes can permit lower concentrations of protein to be used, which can be critically important when investigating large complexes with moderate to low solubility. As a probe of changes in the local environment, the large chemical shift range associated with the ^{19}F shielding parameter allows for better resolution of differences in proteins containing multiple reporting groups. These changes in environment should be particularly evident for ^{19}F probes situated at a binding interface of an antibody−antigen complex. During formation of the complex, changes in the surrounding electric field, short-range contacts, and hydrogen bonding can all potentially affect the observed chemical shift for any ^{19}F nucleus. The atomic radii of ^{1}H and the ^{19}F nucleus are very similar; therefore, when fluorine is substituted on the indole ring of tryptophan, it is not expected to significantly change its shape or space requirements; it is considered a mild structural perturbation when incorporated into proteins. However, the strongly electronegative fluorine nucleus can dramatically alter the charge distribution and dipole moment of an aromatic system compared to hydrogen. The potential utility of the technique is extended by the commercial availability of numerous ^{19}F-labeled amino acids, nucleotides, and sugars that can be biosynthetically incorporated into proteins and/or used for the solid-phase synthesis of small peptides, proteins, RNA, DNA, and polysaccharides. Tryptophan analogues are particularly useful in investigations of larger proteins because the relative abundance of tryptophan in protein sequences is usually much lower than that of other amino acids. This makes assignment of peaks after biosynthetic incorporation less challenging. In addition, antibody−antigen complexes can also reveal information about local changes in flexibility and chemical exchange by measuring NMR relaxation parameters that are influenced by dipole−dipole and chemical shift anisotropy relaxation mechanisms.[12]

Over the past two decades, we and others have studied the HyHEL series of mouse IgG1 antibodies to explore the biophysical and structural changes that accompany affinity maturation to a specific antigen epitope (HEL).[13−32] Crystal structures of representative intermediates along this affinity maturation pathway in complex with HEL have been determined at high resolution and have revealed that binding is enhanced by additional hydrophobic effects and/or interactions and improved shape complementarity.[33] Along with the solid state data, thermodynamic and kinetic data in solution have enhanced our basic understanding of these biologically relevant interactions. Notably, we discovered that when studied by surface plasmon resonance (SPR), some of these complexes follow kinetics of binding much more complex than simple 1:1 association models.[34] Despite this wealth of information, there are several somatic mutations in this series whose physical bases for contributing to changes in binding remain unexplained using these techniques. Furthermore, a comprehensive understanding of a loss of affinity or cross-reactivity to various antigenic mutants remains elusive. This study explores the potential of using ^{19}F NMR of novel scFv antibody analogues, along with X-ray, circular dichroism (CD), and SPR analysis, to reveal new information regarding these interactions. It was thought that the use of various solution techniques may help further illuminate the details of the antibody−antigen binding interactions that may not be resolved in the solid state structures.

In this report, we demonstrate the feasibility and utility of ^{19}F NMR in 1) characterizing the interaction between an intermediate-affinity IgG1 antilysozyme antibody (HyHEL10)[18,35,36] and its antigen and 2) further refining our understanding of physical effects contributing to the binding free energy that are not completely revealed by X-ray analysis alone. We biosynthetically incorporated ^{19}F-labeled tryptophan into a scFv fragment from HyHEL10[13] and analyzed the fluorine spectra of both the free and antigen-complexed analogue-incorporated antibody.

MATERIALS AND METHODS

Sample Preparation. Chemical reagents were purchased from Sigma-Aldrich (St. Louis, MO) unless otherwise indicated. The antigen hen egg white lysozyme (HEL) (Worthington Biochemicals, Lakewood, NJ) was further purified using gel filtration chromatography prior to use. The plasmid containing the wild-type HyHEL10 scFv (hereafter simply termed scFv) antibody construct[13] under control of the T7-lac promoter was transformed into BL21(DE3) cells (EMD Biosciences, San Diego, CA) and expressed as inclusion bodies at 37 °C in LB medium. For complete 5-fluorotryptophan (^{5F}W) incorporation (this scFv termed ^{5F}W-scFv), the plasmid was transformed into the CT19 tryptophan-auxotrophic cell line.[37] For the assignment of NMR peaks to specific tryptophan residues, each tryptophan residue in the scFv sequence was mutated in turn to phenylalanine via site-directed mutagenesis using the Quikchange II Mutagenesis kit (Stratagene, La Jolla, CA). Experimental details of the expression, isolation, and purification of these constructs are outlined in the Supporting Information, including a listing of forward primer sequences used for introducing phenylalanine substitutions (Table S1).

SPR Measurements. Rate constants for affinity determination and thermodynamic parameters were determined using a Biacore 2000 SPR instrument and BIAevaluation (GE Healthcare Bio-Sciences, Piscataway, NJ). Samples were passed over a CM5-dextran chip immobilized with amine-coupled HEL to provide surfaces that ranged from 80 response units (RU) to 150 RU. Previous work has shown that the interaction of this family of antibodies with HEL results in complex two-

step binding kinetics that are best evaluated using a series of different injection times.[38] The SPR experimental protocol consisted of four analyte-inject (association) times of 10, 25, 60, and 120 min, followed by a 2 h dissociation phase with HBS buffer. Data from the corresponding three sensorgrams were corrected using a reference flow cell prepared from the same chip that had been produced using the same amine coupling protocol without protein. These reference-corrected sensorgrams were then pooled for global analysis using a two-step model. Two separate experiments using different concentrations of scFv (18−55 μM) were considered as replicates for statistical analysis.

Thermal Stability Assessment of Proteins. Aggregation due to denaturing for each protein sample was monitored by an increase in absorbance (scattering) at 330 nm (Figure S1 of the Supporting Information). Each sample to be tested was incubated between 25 and 37 °C. At different time intervals, aliquots were removed and diluted to 50 μM prior to measurement of the absorbance at 330 nm. The period of abrupt change in the absorbance profile was used to assess the maximal temperature that could be used for NMR experiments.

X-ray Crystallography. Crystals of scFv and ^{5F}W-scFv were grown by the vapor diffusion method in hanging drops. The complexes with HEL were concentrated to 7.5 mg/mL (scFv) or 2.5 mg/mL (^{5F}W-scFv) in HBS buffer and mixed with a well solution containing 0.2 M sodium citrate and 40% PEG400 in 0.1 M Tris buffer (pH 8.5). Small needle-shaped crystals were grown and used for data collection. Diffraction data extending to 2.3 Å resolution for ^{5F}W-scFv and to 2.7 Å for scFv were recorded at 100 K on beamlines 21-ID-D and 22-BM, respectively, at the Advanced Photon Source (Argonne, IL). For ^{5F}W-scFv, the oscillation range was 0.5° with an exposure time of 0.5 s and a wavelength of 0.979 Å. A Mar-300 detector was used. For scFv, the oscillation range was 0.5° with an exposure time of 2 s and a wavelength of 1 Å. A Mar-225 detector was used. The structure of ^{5F}W-scFv was determined by molecular replacement with PHASER using the structure of a complex of scFv with lysozyme (Protein Data Bank entry 2dqj) as the search model. The structure was initially refined with Phenix, and the refinement was completed with REFMAC. Refinement of scFv was conducted with REMAC using the final coordinates of ^{5F}W-scFv as an initial model. The statistics of refinement for the two structures are listed in Table S2 of the Supporting Information. Structures have been deposited in the Protein Data Bank (http://www.rcsb.org/pdb/home/home.do) as entries 2ZNW (scFv) and 2ZNX (^{5F}W-scFv).

^{19}F NMR. Samples for NMR were prepared immediately prior to use to minimize the possibility of aggregation. HBS-G [10 mM HEPES, 150 mM NaCl, 3 mM EDTA, and 3% (v/v) glycerol (pH 7.4)] was used in preparation of all NMR samples, and glycerol was used in the sample buffer to improve stability and solubility of the sample. Previous work with these antibodies in our lab showed that this level of glycerol does not significantly impact antigen binding and was therefore adequate for the purposes of unambiguously assigning peaks. To each sample was added 10% D_2O as a lock solvent. The scFv antibody labeled with ^{5F}W was concentrated to 350 μM by centrifugation using a prewashed Amicon Ultracel 10000 MWCO spin filter (VWR, West Chester, PA). This was transferred to a clean 1.5 mL centrifuge tube and clarified as necessary at 18000*g* for 10 min at room temperature prior to being loaded into the NMR tube. For titration experiments, HEL was prepared from crystallized, lyophilized powder to a final concentration of 2 mM to limit dilution of the scFv sample during titration. Sample solutions were clarified by centrifugation just prior to use. Phenylalanine mutants were prepared in the same way, but two of these mutants (W36F and W103F) exhibited reduced solubility during concentration.

^{19}F NMR spectra were recorded using a Varian (Palo Alto, CA) INOVA 500 spectrometer operating at 470 MHz using a specially designed H-F probe with a single channel dual-tuned to both ^{1}H and ^{19}F (Nalorac). All NMR experiments were performed at 30 °C unless otherwise noted (vide infra). The ^{19}F resonances were referenced to trifluoroacetic acid (TFA) at −76.55 ppm as an external standard. Because of the low concentration, experiments were conducted for a minimum of 5000 increments to obtain spectra with a sufficient signal-to-noise ratio (S/N). Most spectra of the complex were run overnight with standard one-dimensional pulse sequences. Longitudinal (T_1) and transverse (T_2) relaxation time measurements were taken using inversion−recovery and Carr−Purcell−Meiboom−Gill (CPMG) spin echo pulse sequences, respectively, taken from the Varian Chempack sequence library within VNMRJ version 2.2d. Relaxation times were calculated using macros defined in the Varian software. The lengths for the 90° and 180° pulses in the T_2 experiments were 14 and 28 μs, respectively. The time between consecutive 180° pulses (τ_{cp}) ranged from 0.12 to 1 ms for the inspection of the variation of T_2 with τ_{cp}.

RESULTS AND DISCUSSION

Incorporation of ^{5F}W into scFv and Characterization. Several fluorinated and mutant scFv proteins were prepared (for detailed experimental procedures and forward primer sequences, see the Supporting Information and Table S1). A total of 14 proteins were prepared; these are listed in Table 1: wild-type scFv, "fully" fluorinated protein ^{5F}W-scFv (all six tryptophans replaced with ^{5F}W), six ^{5F}W-scFv analogues in which each of the six ^{5F}W residues was individually replaced with a single phenylalanine residue [designated ^{5F}W(Phe*X*)-scFv, where *X* is the residue number of the mutation], and six nonfluorinated proteins in which each tryptophan was individually mutated in turn to a phenylalanine [designated (Phe*X*)-scFv, where *X* is the residue number of the mutation]. The phenylalanine mutants were prepared to aid in both the assignment of the fluorinated residues by NMR and the assessment of the effect each fluorinated tryptophan had on the binding of the scFv to HEL antigen (vide infra).

With the exception of the light chain mutant ^{5F}W(Phe35)-scFv, all antibodies were successfully refolded and purified to yield stable soluble material. The ^{5F}W(Phe35)-scFv antibody showed weakened binding to the anion exchange column, eluting at a much lower concentration of NaCl during the gradient. This mutant also exhibited significant amounts of soluble protein aggregate that eluted in the void volume during gel filtration chromatography indicative of incomplete or poorly refolded scFv. The tryptophan at this position is invariant in IgG sequences and is likely critical to IgG folding and stability. All purified antibodies were functional and bound to HEL as assessed by SPR (see below), with the exception of ^{5F}W-(Phe35)-scFv. Both the ^{5F}W(Phe35)-scFv and (Phe35)-scFv samples exhibited poor reproducibility with successive kinetic runs reflecting sample instability. Data for these samples were excluded when comparing results for other mutants.

The ^{5F}W-scFv liquid chromatography−mass spectrometry analysis showed a single peak with one molecular ion

Table 1. Antibodies Prepared in This Study and Their SPR-Derived Antigen Binding Affinities

entry	antibody	description	K_D (nM)
1	scFv	wild-type protein	0.130
2	^{5F}W-scFv	all Trp residues substituted with fluorine	4.03
3	(Phe35)-scFv[a]	same as scFv, with the Trp35Phe mutation	NA[c]
4	^{5F}W(Phe35)-scFv[a]	same as ^{5F}W-scFv, with the Trp35Phe mutation	NA[c]
5	(Phe94)-scFv[a]	same as scFv, with the Trp94Phe mutation	0.272
6	^{5F}W(Phe94)-scFv[a]	same as ^{5F}W-scFv, with the Trp94Phe mutation	1.99
7	(Phe34)-scFv[b]	same as scFv, with the Trp34Phe mutation	0.266
8	^{5F}W(Phe34)-scFv[b]	same as ^{5F}W-scFv, with the Trp34Phe mutation	1.22
9	(Phe36)-scFv[b]	same as scFv, with the Trp36Phe mutation	0.559
10	^{5F}W(Phe36)-scFv[b]	same as ^{5F}W-scFv, with the Trp36Phe mutation	4.22
11	(Phe98)-scFv[b]	same as scFv, with the Trp98Phe mutation	1.45
12	^{5F}W(Phe98)-scFv[b]	same as ^{5F}W-scFv, with the Trp98Phe mutation	1.25
13	(Phe103)-scFv[b]	same as scFv with the Trp103Phe mutation	0.113
14	^{5F}W(Phe103)-scFv[b]	same as ^{5F}W-scFv, with the Trp103Phe mutation	3.52

[a]Light chain residues. [b]Heavy chain residues. [c]Data not available because of instability.

corresponding to 26369.8 Da, indicating that each of the six naturally occurring tryptophan positions has been replaced with ^{5F}W. No other peaks that corresponded to other fluorinated species could be identified; therefore, the level of incorporation was presumed to be 100%.

Crystal Structures. As in our previous studies,[33] we examined the crystal structures of both the wild-type scFv fragment and its fully fluorinated analogue in complex with HEL. Although uncomplexed single-chain antibody fragments can be analyzed by crystallography,[39,40] this remains difficult because of the inherent flexibility of these constructs. The uncomplexed scFv prepared here could not be analyzed, but moderate-resolution structures were obtained for both the wild-type and ^{5F}W-incorporated scFv complexes with HEL. Figure 1A shows a depiction of the antibodies in complex with HEL highlighting the tryptophan residues in the scFv that were modified with fluorine. The crystallographic data and statistics are listed in Table S2 of the Supporting Information. Two antibody molecules and two lysozyme molecules were present in the crystal asymmetric unit.

The overall quality of the models, as assessed by PROCHECK[41] and by other parameters such as R factors, meets the acceptable criteria for structures determined with comparably limited resolution of the diffraction data.[42,43] All main chain atoms and most of the side chains fit well into the $2F_o - F_c$ electron density map. The quality of the $F_o - F_c$ electron density map (Figure 1B) is also quite good, defining their conformation in an unambiguous manner.

Superposition of the two independent antibody molecules in the wild-type structure results in a root-mean-square deviation (rmsd) of 0.65 Å for 220 Cα atoms. Simultaneous superposition of the two complexes of the wild-type and fluorinated antibody resulted in an rmsd of 0.34 Å for 700 Cα atoms, whereas a similar comparison of only "A" molecules from the asymmetric unit of the antibodies yielded an rmsd of 0.24 Å for 221 Cα atoms. The latter value is within the range of structure accuracy expected at this resolution, whereas superposition of two crystallographically independent molecules includes structural changes due to crystal packing.

All tryptophan residues in the wild-type antibody and ^{5F}W residues in the variant are very well ordered. When the wild-type and fluorinated complexes are superimposed as discussed above, the side chains of these residues are almost completely superimposable, with the largest deviation between corresponding atoms not exceeding 0.3 Å. Because that variation is very similar to the accuracy of the structures themselves, we can conclude that modification of the tryptophan side chains did not lead to any significant changes in the static structures of these proteins. In Figure 1C, the three panels show expanded views along with the charge density depiction of ^{5F}W residues 34, 94, and 98 (red) in an overlay with the wild-type complex (green) and include nearby residues from the antigen (gray). These residues are at or near the interface of the antibody–antigen complex. These orientations showcase some of the potential charge–charge interactions introduced with the fluorinated amino acids. The electronegative fluorine atom causes a distinct change to the dipole moment and charge distribution of the tryptophan indole ring[44] that could result in either positive or negative contributions to binding. In this case, the effect is detrimental because the ^{5F}W-scFv–HEL association has a lower affinity than the wild-type complex (vide infra).

Circular Dichroism and UV. A comparison of the UV and CD spectra of scFv and ^{5F}W-scFv is shown in Figure 2. The small red shift of the absorbance maximum that is typically characteristic for ^{5F}W-modified proteins was also observed for our fully fluorinated analogue, ^{5F}W-scFv[45] (Figure 2A). The CD spectrum of ^{5F}W-scFv also showed small but significant shifts relative to its unfluorinated counterpart, indicating a change in secondary structure with ^{5F}W incorporation. The wild-type scFv displays a more typical β-like signature; the spectrum of ^{5F}W-scFv was more disordered, with the negative band at 218 nm slightly blue-shifted with a lower ellipticity. Hence, Figure 2B suggests that slightly different conformations are preferred in solution for the wild-type and fluorinated scFv analogues. This slight change in the overall conformation is translated to the complex structures with HEL, as shown by the comparison of the CD data for wild-type and ^{5F}W-scFv complexes (Figure 2C). Despite the results that show virtually indistinguishable HEL structures, this is likely not the case for complex structures in solution (vide infra).

Binding Kinetics Using Biacore SPR. Previous work using SPR has shown that the interaction of this family of antibodies with HEL results in complex two-step binding kinetics (eq 1) that are best evaluated using a series of different injection times.[38]

$$A + B \underset{k_{-1}}{\overset{k_1}{\rightleftarrows}} AB \underset{k_{-2}}{\overset{k_2}{\rightleftarrows}} AB^* \quad (1)$$

where AB is the intermediate encounter complex and AB* is the final docked conformation. This protocol derives from the observation that the kinetics of dissociation of the antibody from bound antigen on the surface of the chip is dependent on the length of time used for association. The longer the injection time, the more stable the complex. Furthermore, the forward

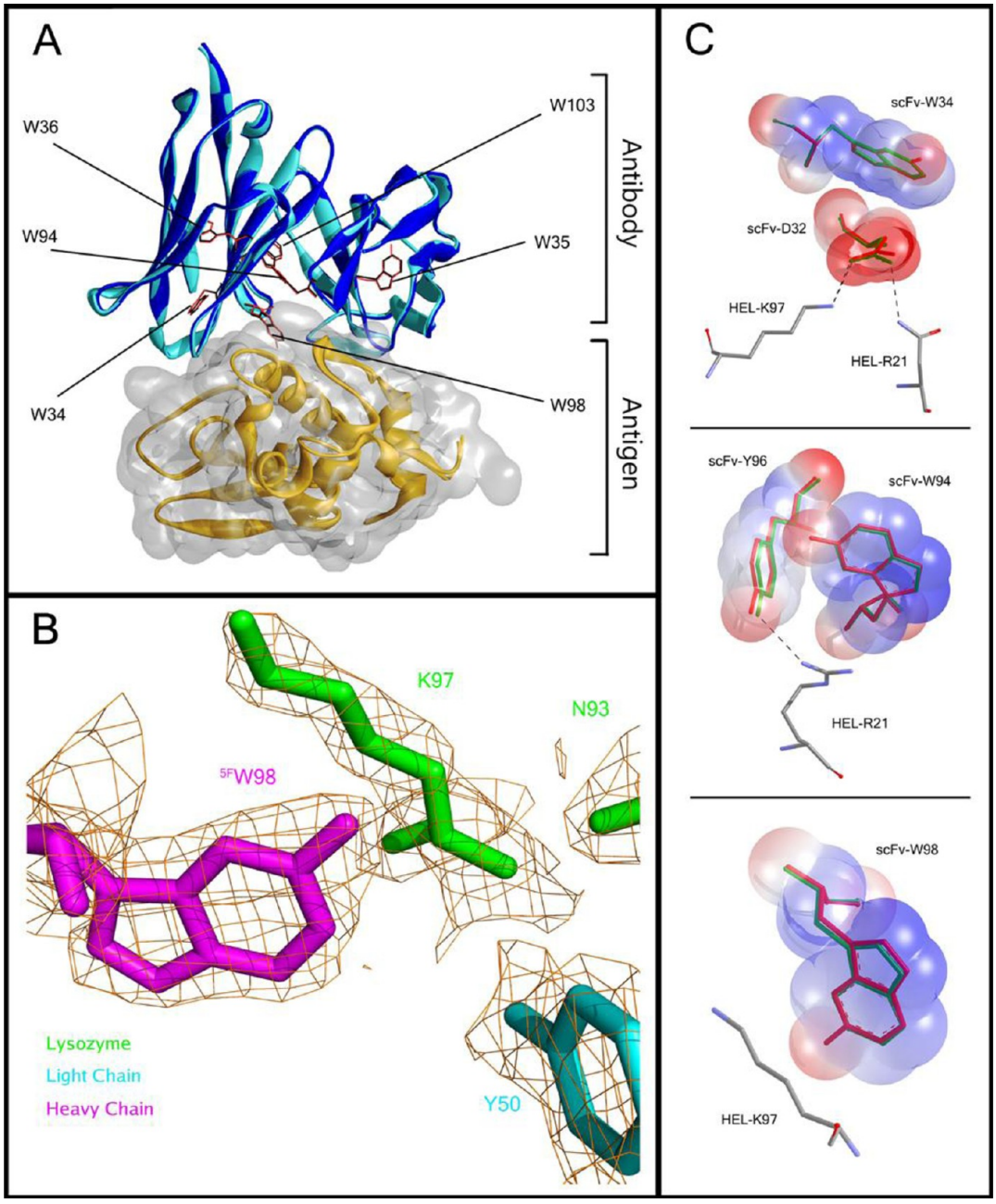

Figure 1. Crystal structures of the antibody–HEL complexes. (A) Ribbon depiction of the crystal structure of the scFv–HEL complex overlaid with ^{5F}W-scFv. Antibodies are colored dark blue and cyan, and HEL is colored yellow. The two structures are virtually superimposable. The six modified tryptophan residues are annotated. (B) Depiction of the $F_o - F_c$ electron density map at the antibody–HEL interface (antibody colored purple, HEL colored green) showing the quality of the X-ay data. (C) Expansions of three key tryptophan residues in the overlay of the complex from panel A. The unmodified scFv is colored green and ^{5F}W-scFv red, and HEL residues are colored gray. These magnifications show any possible steric or electronic influence on the interaction with specific HEL residues.

rate constant for the second step (k_2) is concentration-independent. These two observations are consistent with a model in which there is a structural change in the antibody (A)–antigen (B) complex over the time course of association that in turn affects the observed off rate. The antibody (A) and antigen (B) form an initial encounter complex (AB) followed by an additional conformational rearrangement resulting in the more stable docked conformer (AB*). One experimental SPR cycle can sample only a specific population during the course of this time-dependent structural change. Therefore, it is necessary to measure dissociation after several different times of association to better represent the two bound states in the final global fit. A summary of the binding constants derived from SPR kinetic experiments for all samples is presented in Table 1.

When ^{5F}W is incorporated into each of the six tryptophan positions in scFv, the affinity is as much as 31 times lower than that of the same antibody without ^{5F}W substitution (Table 1, entries 1 and 2, and Figure 3). Despite the antibody still having strong nanomolar affinity for antigen, this large decrease in affinity with fluoro analogue incorporation was surprising. Upon comparison of the affinities of the phenylalanine mutants,

dx.doi.org/10.1021/bi300455t | *Biochemistry* 2012, 51, 6017–6027

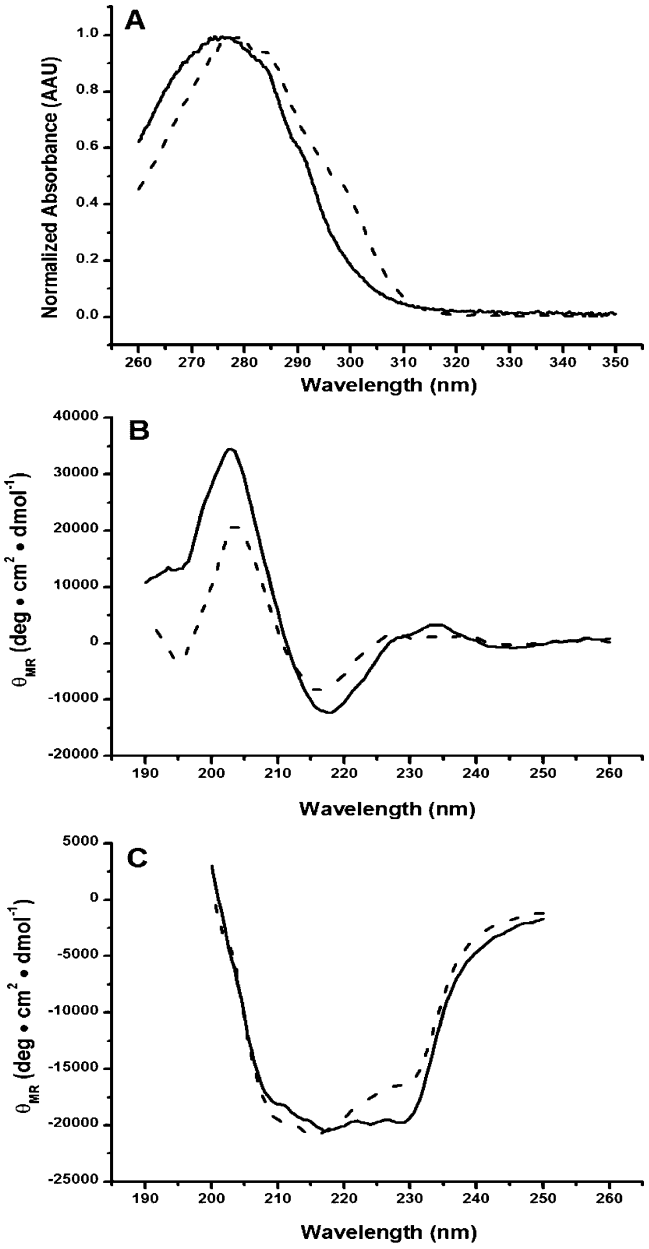

Figure 2. Comparison of the (A) UV spectra normalized to the absorption maximum and (B) CD spectra for scFv (—) and ^{5F}W-scFv (---). (C) Comparison of CD data for the scFv–HEL (—) and ^{5F}W-scFv–HEL (---) complexes.

an increase in the level of binding with this substitution relative to that with ^{5F}W at that position indicates the degree of impact that the analogue is having on binding to HEL. The ^{5F}W-(Phe36)-scFv mutant (entry 10) showed binding very similar to that of ^{5F}W-scFv, indicating that substitution of 5-fluorotryptophan at this position had very little impact on binding. Both the ^{5F}W(Phe94)-scFv (entry 6) and ^{5F}W-(Phe98)-scFv (entry 12) mutants had higher binding affinity than ^{5F}W-scFv and, therefore, negatively impacted binding to HEL. With positions 94 and 34, the mutation to phenylalanine at that position in the wild-type protein [(Phe94)-scFv and (Phe34)-scFv, entries 5 and 7, respectively] had very little impact on binding (~2-fold); however, at position 98, the same phenylalanine substitution [(Phe98)-scFv, entry 11] resulted in a binding affinity that was very similar to that observed with the

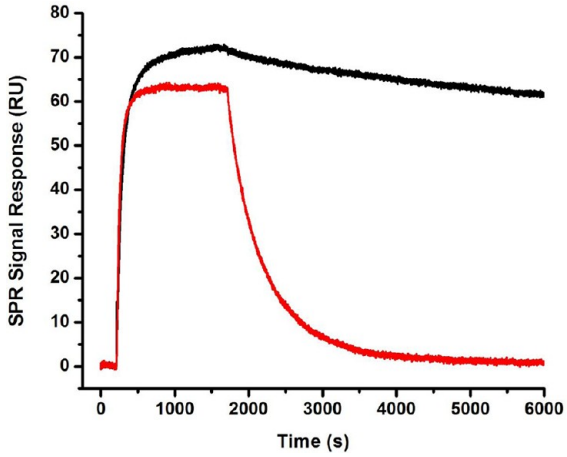

Figure 3. Impact of complete tryptophan replacement with ^{5F}W on antibody–antigen interaction. SPR sensograms of scFv (black) and ^{5F}W-scFv (red). The antigen was immobilized on a carboxymethyl dextran chip surface via amine coupling, and binding (response) was monitored as the antibody was injected over this surface at a flow rate of 10 μL/min. Curves represent comparisons of one time course for injection with a group of four different injection times.

same mutation and ^{5F}W incorporated at the other five positions [^{5F}W(Phe98)-scFv, entry 12]. It can be expected that with ^{5F}W(Phe98)-scFv, the phenylalanine substitution would have a similar negative impact on binding; this must be taken into account when judging the relative impact of ^{5F}W at position 98. Essentially no effect on binding was observed upon replacement of position 103 with phenylalanine (entry 13), whereas mutation of W103 to Phe in the fully fluorinated protein (entry 14) had a small positive effect on binding of HEL by SPR.

Optimal Conditions for and Peak Assignments from ^{19}F NMR Experiments. To determine the optimal temperature for NMR experiments, the thermal stability of ^{5F}W-incorporated antibody samples was determined by measuring absorbance changes (scattering) at 330 nm as a result of unfolding and aggregation (Figure S1 of the Supporting Information). This was performed at concentrations comparable to those that could be expected for the NMR experiments (approximately 300 μM). At 37 °C, the ^{5F}W-scFv antibody was not stable over the 16 h incubation period and showed significant signs of aggregation after 2 h. As the temperature is lowered, stability increases, and at 30 °C, the antibody shows very little indication of aggregation. This was the temperature chosen to perform all NMR experiments.

A total of six fluorine peaks were expected for the modified antibody corresponding to the six tryptophans present in its primary sequence (and later confirmed by mass spectrometry) that were replaced with ^{5F}W. For the uncomplexed ^{5F}W-scFv, a series of broad, semiresolved peaks were observed at 30 °C (Figure 4). Varying conditions produced limited success. For resonance assignment, each tryptophan was mutated to phenylalanine in the ^{5F}W-scFv construct, resulting in five ^{19}F peaks; however, like the wild-type protein, each mutant in its free (uncomplexed) form was not fully resolved, and in some cases, not all peaks were observed (representative examples are shown in Figure 4B–D).

When ^{5F}W-scFv was titrated with HEL, a gradual separation of all six peaks was observed and all were clearly distinguishable at a 1:1 ratio (Figure 5). Importantly, three peaks showed large

dx.doi.org/10.1021/bi300455t | Biochemistry 2012, 51, 6017–6027

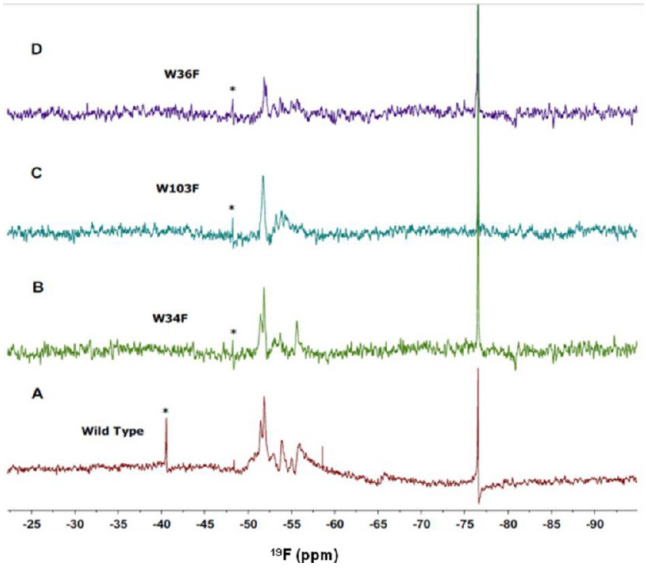

Figure 4. One-dimensional ^{19}F NMR solution spectra of (A) ^{5F}W-scFv (wild type, all six tryptophans labeled) and (B–D) three single-phenylalanine mutants (five labeled tryptophans) showing the poor sensitivity and peak overlap in the free modified antibodies. The peak marked with an asterisk is an unidentified impurity that was in all samples.

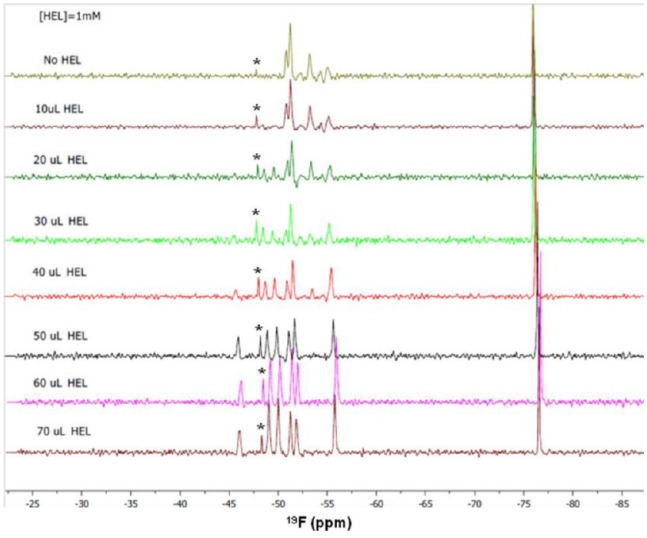

Figure 5. Titration of increasing amounts of HEL into ^{5F}W-scFv (top to bottom traces). The resolution of all peaks is clear at a 1:1 ^{5F}W-scFv:HEL ratio. The peak marked with an asterisk is an unidentified impurity that was in all samples.

changes in the chemical and magnetic environment upon complex formation. Interestingly, in the free scFv construct, all peaks show increased levels of line broadening, indicating the possible presence of several conformational subpopulations. Via comparison of the $T = 0$ spectra [no HEL (Figure 5)] of ^{5F}W-scFv and the Phe mutants with those of their complexes, most peaks were unambiguously assigned to a specific ^{5F}W. As expected, the spectrum of these mutant complexes showed only five peaks with the missing peak corresponding to the phenylalanine-substituted position (Figure 6A). Only five mutants (see Table 1) were used, because of the aforementioned folding and stability issues with the W35F construct. Assignments for residues 38, 94, 98, and 103 were relatively

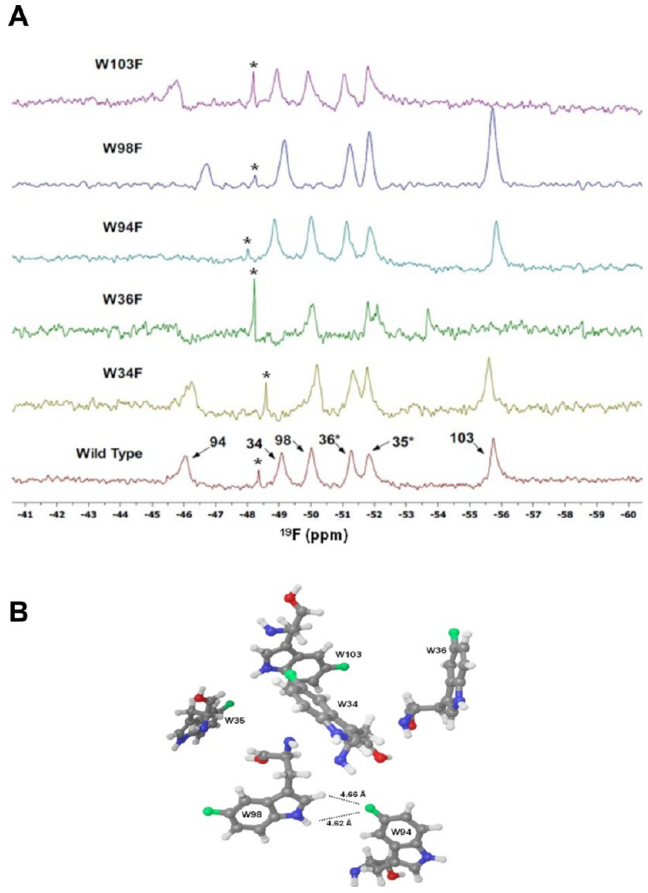

Figure 6. Assignment of fluorine signals in ^{5F}W-scFv. (A) Stacked spectra of the complex structures of ^{5F}W-scFv with HEL and several Phe mutants with HEL. Assignments are annotated in the spectrum of the ^{5F}W-scFv–HEL complex (bottom). The asterisk on W35 and W36 indicates that we were not able to unequivocally assign each of these peaks, and thus, their chemical shifts may be interchanged. (B) Expansion of the six ^{5F}W residues from the complex crystal structure in Figure 1A depicting the possible chemical and magnetic influence specific phenylalanine mutants may have on the fluorine chemical shift of nearby ^{5F}W. The singlet peak marked with an asterisk is an unidentified impurity that was in all samples.

straightforward. The W36F spectrum was difficult to interpret, as the resolution and sensitivity (Figure 6A) were lower than expected, making this and the W35F residue assignment tentative. The solid and tentative assignments, based on the collected data, are shown in the bottom spectrum of Figure 6A. Also notable was the fact that in the single-Phe mutants of ^{5F}W-scFv, there were distinctive chemical shift changes in some of the remaining fluorine signals. A diagnostic example is W98F mutant ^{5F}W(Phe98)-scFv: In this mutant, the ^{5F}W94 signal experiences a significant upfield shift because of the change to phenylalanine. When position 98 is a tryptophan, the indole NH and H2 protons are within 4.6 Å of the ^{5F}W94 fluorine atom (Figure 6B). A change from indole to phenyl could adjust the aromatic ring such that ^{5F}W94 is shielded relative to ^{5F}W-scFv. There are also noticeable downfield shifts for ^{5F}W94 in the ^{5F}W103F mutant. The fact that these two residues are not in the proximity of each other suggests a more "global" conformational adjustment in response to the ^{5F}W103F mutation, again affecting ^{5F}W94. The results show that interfacial residues W94 and W98 are critical determinants of the structural integrity of the complex.

dx.doi.org/10.1021/bi300455t | *Biochemistry* 2012, 51, 6017–6027

^{19}F Relaxation Analysis. To qualitatively define the dynamic environment of the fluorinated tryptophans and possible chemical exchange phenomena, the T_1 and T_2 relaxation times were calculated for each of the six ^{5F}W residues in the ^{5F}W-scFv−HEL complex. Table 2 lists the calculated T_1 and T_2 values for each residue, as well as T_2 values obtained by varying the τ delay that separates the two 180° pulses in the CPMGT2 sequence (so-called τ_{cp} in the Varian pulse sequence). If the relaxation times vary with different values of τ_{cp}, one can conclude that a chemical exchange is taking place between the ligand and receptor.[46,47]

Table 2. Longitudinal (T_1) and Transverse (T_2) Relaxation Times for ^{5F}W-Substituted Residues in ^{5F}W-scFv

peak (low to high field)	T_1[a]	T_2[a] (0.12 ms)[b]	T_2[a] (0.5 ms)[b]	T_2[a] (1 ms)[b]
1(94)[c]	1198	1.27	3.84	4.12
2(34)[c]	1742	1.85	4.39	4.08
3(98)[c]	1144	1.57	4.88	4.94
4(35)[c,d]	795	1.35	5.97	5.03
5(36)[c,d]	1171	1.54	5.77	4.29
6(103)[c]	1236	1.72	5.99	4.44

[a]Times in milliseconds. [b]Values in parentheses are the Tau delays in the CPMGT2 pulse sequence. [c]Values in parentheses are residue numbers assigned from the spectra. [d]Tentative assignment.

Values of both spin−lattice (T_1) and spin−spin (T_2) relaxation are in the ranges that have been observed for fluorinated amino acids incorporated into protein complexes of a similar size.[12] The majority of T_1 values are slightly over 1 s, with the exception of that of W35 (795 ms). As shown in Table 2 and Figure 6A, it was not possible to differentiate between tryptophans 35 and 36 because the W35F mutant was not sufficiently stable for NMR analysis. However, the lower T_1 may be a clue about the identity of W35 because the ^{5F}W side chain of this residue is buried between strands of two β-sheets of the scFv structure in the solid state, whereas W36 is more exposed to the solvent (vide infra).

As stated above, it is possible to detect exchange phenomena and to potentially assign specific processes by adjusting parameters in the CPMG sequence. According to relationships (derived from the original Bloch equations) postulated by Luz and Meiboom[48,49] and further refined by Allerhand and Gutowsky[50] along with Carver and Richards,[46] as the 180° interpulse delay is increased, there is a corresponding increase in the T_2 relaxation rate:

$$1/T_2 = 1/T_2^\circ + P_a P_b(\delta\omega)^2\tau[1 - (2\tau/\tau_{cp})\tanh(\tau_{cp}/2\tau)] \quad (2)$$

where T_2° is the value of T_2 at which no exchange takes place, P_a and P_b are the fractional proportions of the molecules in states a and b, respectively, and τ_{cp} is the interval between 180° pulses. It is assumed that chemical exchange is limited to two sites and the spin echo decay in the experiment is exponential. Only a handful of studies have utilized this concept in attempts to define various aspects of exchange phenomena, and they have primarily dealt with small molecule ligand binding.[48,49,51] One specific report utilized ^{19}F NMR to define a chemical exchange process related to different small drug molecules bound to a ^{5F}W-labeled ionotropic glutamate receptor, GluR2.[52] According to eq 2, T_2 decreases as the interpulse delay τ_{cp} is increased; this was observed for a specific ^{5F}W residue in ref 52. In the case of the ^{5F}W-scFv complex with HEL, there is a dramatic increase in T_2 values with an increasing τ_{cp}. In addition, all ^{5F}W residues experience this increase in T_2 and in approximately equal amounts. This suggests a global exchange phenomenon occurring on the time scale of the interpulse delay that (1) is not localized near one or two specific residues and (2) serves to depress the relaxation rate rather than increase it as suggested by eq 2. The suggestion here is that the motion that is sampled during the CPMG experiment is one in which the fluorine atoms experience "less ability" to interact with other spins, possibly indicating some momentary loss of well-defined tertiary structure. However, this proposal would stand in contrast with the fact that although the ^{5F}W-scFv−HEL complex has a binding affinity lower than that of the wild type, there remains relatively strong binding (binding constants still in the nanomolar range). In addition, after the initial "jump" in relaxation time, the last point suggests perhaps a modest decrease in T_2, which more accurately fits the theory and eq 2. As only three data points were collected because of the mild loss of stability (and hence sensitivity) with time, an accurate depiction of the actual exchange process occurring during these experiments could not be developed. These data point to the complexity of the changes occurring in our system in solution.

Relevant Effects of Incorporation of ^{19}F into HyHEL10 scFv. We had prepared mutant scFv constructs in which all tryptophans are replaced with ^{5F}W as well as those with single-Phe replacements leaving five fluorine atoms for the purposes of assignment. In addition, nonfluorinated mutants in which each tryptophan was replaced with Phe in the wild-type antibody were prepared. A comparison of the $\Delta\Delta G$ values calculated from the kinetically derived (SPR) binding constants is useful in defining the contributions that each individual fluorine-containing residue makes to the overall antigen−antibody binding of the fully fluorinated antibody, ^{5F}W-scFv. An illustration of this analysis is shown in Figure 7 and Table 3. The value of $\Delta\Delta G$ for ^{5F}W-scFv relative to scFv is 1.97 kcal/mol. If the $\Delta\Delta G$ from ^{5F}W-scFv where one tryptophan is mutated is calculated and subtracted from 1.97, a qualitative measure of the contribution of each ^{5F}W on that specific residue is obtained. As seen in Table 3, major differences exist for W94, W98, and W34. Several lines of data (vide supra) confirm the influence of W94 and W98. W34 is positioned at the edge of a β-strand on the heavy chain that begins a loop connecting another strand of a β-sheet. The integrity of that loop may be compromised by mutation of this residue and in turn affect the formation of proper secondary structure, which weakens binding. Furthermore, the W34 indole makes contact with Asp32 (Figure 1C). Asp32 in turn is involved in two important salt bridges with antigen hot-spot residues Arg21 and Lys97. A change in charge distribution in the neighboring W34 may influence this charge−charge interaction between Asp21 and the hot-spot residues. In addition, W98 makes an energetically important contact with HEL; it is involved in both hydrogen bonding and a salt-link network.[28] The partial charge change at that position due to the modified dipole moment of the fluorinated indole ring in ^{5F}W, together with the overall change in hydrophobicity with this tryptophan analogue, may explain the observed change in function. Finally, Figure 6A depicts the detrimental effect that particular substitutions have on both the sensitivity of the NMR spectra and broadening of peaks; some virtually disappear, viz., the W103 signal in the W36F spectrum. Close examination of the structures reveals

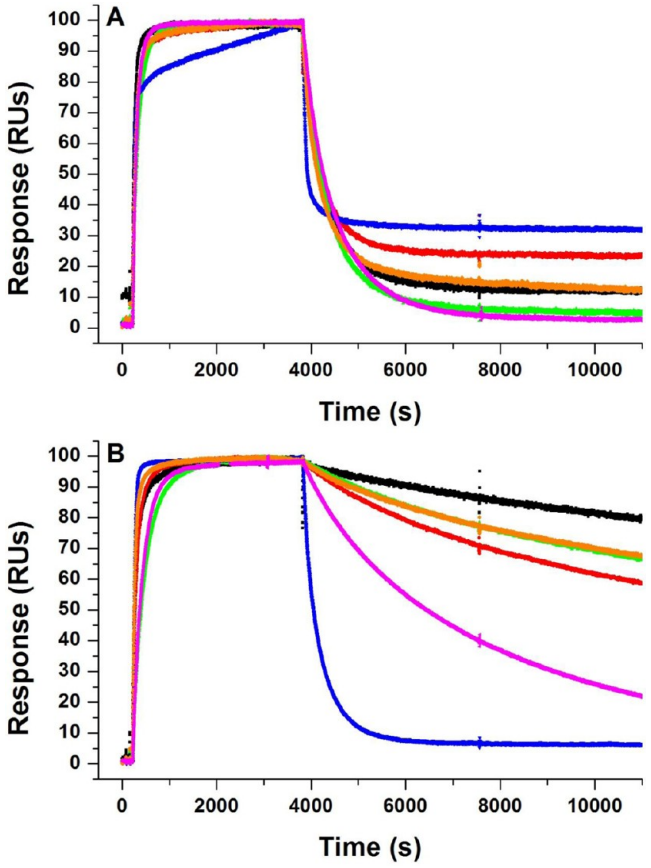

Figure 7. Impact of single tryptophan to phenylalanine mutations and ^{5F}W incorporation on antibody−antigen interaction. SPR single-cycle sensorgrams are provided and were normalized to the starting point for dissociation for comparison. (A) Single-phenylalanine substitutions with ^{5F}W biosynthetically incorporated at the five other tryptophan positions: ^{5F}W-scFv (black), ^{5F}W(Phe34)-scFv (red), ^{5F}W(Phe98)-scFv (blue), ^{5F}W(Phe36)-scFv (green), ^{5F}W(Phe103)-scFv (orange), and ^{5F}W(Phe94)-scFv (magenta). (B) Single-phenylalanine subsitutions with no ^{5F}W incorporation: scFv (black), (Phe34)-scFv (red), (Phe98)-scFv (blue), (Phe36)-scFv (green), (Phe103)-scFv (orange), and (Phe94)-scFv (magenta).

Table 3. Effect of Each Individual Fluorinated Residue on the Overall Binding of ^{5F}W-scFv to HEL

antibody	$\Delta\Delta G_1{}^a$	$\Delta\Delta G_2{}^b$	$\Delta\Delta G_3{}^c$
scFv			
^{5F}W-scFv		1.97	
(Phe94^a)-scFv	1.47		
^{5F}W(Phe94^a)-scFv		0.77	1.20
(Phe34^b)-scFv	0.71		
^{5F}W(Phe34^b)-scFv		0.9	1.07
(Phe36^b)-scFv	1.15		
^{5F}W(Phe36^b)-scFv		1.88	0.10
(Phe98^b)-scFv	1.63		
^{5F}W(Phe98^b)-scFv		0.35	1.62
(Phe103^b)-scFv	0.20		
^{5F}W(Phe103^b)-scFv		2.04	−0.07

^{a}Difference between unlabeled and single-Phe mutants. ^{b}Difference between unlabeled and labeled antibody for each mutant. ^{c}Contribution of incorporation of ^{5F}W into the specific Trp position.

that W36 is sandwiched between two β-sheets, with W103 positioned on a long loop connecting two strands of one of the sheets of the sandwich. There is an obvious disruption in the interfacial contacts by a W36F mutation, compromising the structural integrity of much of the heavy chain. This in effect may cause W103 to be much more mobile, resulting in a severely broadened peak that cannot be observed under the conditions of the experiment.

For this work, we were interested in comparing differences in interactions between a model scFv and its fluorinated analogues and HEL, within the context of the modified antibody. Evidence that these fluoroindole derivatives do not significantly impact the structure of the complex was found for the solid state. While CD experiments suggested some small changes in structure for the free antibody, SPR measurements clearly indicate that there is a distinct change in function for the antibody analogue that is highly site-dependent. Our results support the observation that these analogues can affect function, so care must always be taken when extrapolating results to the wild-type protein. In addition, as there did not seem to be any obvious deleterious steric or hydrogen bonding influences of fluorine incorporation, the aforementioned change in the dipole moment could explain the lower overall affinity and possible exchange phenomena in this system. Incorporation of 4-fluorotryptophan (^{4F}W) residues, whose indole dipole moment is similar to that of unmodified indole, into scFv resulted in an affinity with HEL (by SPR) that was similar to that of the wild-type protein (data not shown). Although the level of incorporation of ^{4F}W was lower than that of ^{5F}W and hence no high-resolution structures were obtained, the data do suggest that the ^{5F}W dipole moment is the critical property that affects the properties of binding to the antigen. Thus, although irreplaceable in structural biology, X-ray crystal structures are often insufficient for unambiguously assessing the impact of changes introduced by specific analogues in a protein.

CONCLUSION

^{19}F NMR data obtained from incorporating 5-fluorotryptophan into a scFv antibody have provided valuable insights into the environment around these reporting groups at the binding interface and the changes that occur from the free antibody. It also illustrates that the function of the residue may influence the impact of a ^{19}F substitution when it is done in isolation. To the best of our knowledge, this is the first report of intrinsic labeling of an antibody with NMR active fluorinated amino acids for use in NMR analysis. These data can be used to better interpret the physical impact of somatic and antigenic mutations and better inform engineering efforts to modify binding to mutants. Future studies should include looking at other mutations at the interface targeted around the reporting groups, using other fluorotryptophan probes to compare and contrast their possible impact on binding, and assessing the introduction of additional tryptophan positions into the antibody sequence at the binding interface to act as new reporting groups.

ASSOCIATED CONTENT

Supporting Information

Experimental procedures for protein expression, tables with forward primers used for phenylalanine substitution mutants, crystallographic statistics, and refinement data, and light scattering experiments that aimed to determine the optimal

dx.doi.org/10.1021/bi300455t | Biochemistry 2012, 51, 6017−6027

temperature for NMR experiments. This material is available free of charge via the Internet at http://pubs.acs.org.

AUTHOR INFORMATION

Corresponding Author

*J.J.B.: Chemical Biology Laboratory, Center for Cancer Research, Frederick National Laboratories for Cancer Research, Bldg. 376, Room 209, Frederick, MD 21702-1201; e-mail, barchi@helix.nih.gov; phone, (301) 846-5905; fax, (301) 846-6033. S.S.-G.: Structural Immunology Section, Structural Biophysics Laboratory, Center for Cancer Research, National Cancer Institute-Frederick, Bldg. 538, Room 167, Frederick, MD 21702-1201; e-mail, sandrasmithgill@aol.com; phone, (301) 846-5203.

Present Addresses

[⊥]Department of Medicinal Chemistry, University of Washington, Seattle, WA 98195.

[@]Lombardi Comprehensive Cancer Center, Georgetown University Medical Center, Washington, DC 20007.

[#]Department of Biochemistry and Biophysics, Perelman School of Medicine at The University of Pennsylvania, Philadelphia, PA 19104.

[▽]Center for Biotechnology and Interdisciplinary Studies, Rensselaer Polytechnic Institute, Troy, NY 12180.

[●]Center for Pharmaceutical Biotechnology and Department of Medicinal Chemistry and Pharmacognosy, The University of Illinois at Chicago, Chicago, IL 60607.

Funding

This work was supported in part by the Intramural Research Program of the National Institutes of Health, National Cancer Institute, Center for Cancer Research, and federal funds from the National Cancer Institute, National Institutes of Health, under Contract HHSN261200800001E.

Notes

The authors declare no competing financial interest.

ACKNOWLEDGMENTS

We thank the Biophysics Resource of the Structural Biology Laboratory at the Frederick National Laboratory for Cancer Research. Use of the Advanced Photon Source was supported by the U. S. Department of Energy, Office of Science, Office of Basic Energy Sciences, under Contract Nos. W-31-109-Eng-38 and DE-AC02-06CH11357. Data were collected at Southeast Regional Collaborative Access Team (SER-CAT) 22-BM beamline at the Advanced Photon Source, Argonne National Laboratory. Supporting institutions may be found at www.ser-cat.org/members.html. Use of the LS-CAT Sector 21 was supported by the Michigan Economic Development Corporation and the Michigan Technology Tri-Corridor for the support of this research program (Grant 085P1000817).

REFERENCES

(1) Braden, B. C., and Poljak, R. J. (1995) Structural Features of the Reactions between Antibodies and Protein Antigens. *FASEB J. 9*, 9–16.

(2) Otlewski, J., and Apostoluk, W. (1997) Structural and energetic aspects of protein-protein recognition. *Acta Biochim. Pol. 44*, 367–387.

(3) Lo Conte, L., Chothia, C., and Janin, J. (1999) The atomic structure of protein-protein recognition sites. *J. Mol. Biol. 285*, 2177–2198.

(4) Davies, D. R., and Cohen, G. H. (1996) Interactions of protein antigens with antibodies. *Proc. Natl. Acad. Sci. U.S.A. 93*, 7–12.

(5) Ramsland, P. A., and Farrugia, W. (2002) Crystal structures of human antibodies: A detailed and unfinished tapestry of immunoglobulin gene products. *J. Mol. Recognit. 15*, 248–259.

(6) Dall'Acqua, W., Goldman, E. R., Lin, W. H., Teng, C., Tsuchiya, D., Li, H. M., Ysern, X., Braden, B. C., Li, Y. L., Smith-Gill, S. J., and Mariuzza, R. A. (1998) A mutational analysis of binding interactions in an antigen-antibody protein-protein complex. *Biochemistry 37*, 7981–7991.

(7) Tsang, P., Rance, M., and Wright, P. E. (1991) Isotope-Edited Nuclear-Magnetic-Resonance Studies of Fab Peptide Complexes. *Methods Enzymol. 203*, 241–261.

(8) Wright, P. E., Dyson, H. J., Lerner, R. A., Riechmann, L., and Tsang, P. (1990) Antigen-Antibody Interactions: An NMR Approach. *Biochem. Pharmacol. 40*, 83–88.

(9) Tsang, P., Rance, M., Fieser, T. M., Ostresh, J. M., Houghten, R. A., Lerner, R. A., and Wright, P. E. (1992) Conformation and Dynamics of an Fab′-Bound Peptide by Isotope-Edited NMR-Spectroscopy. *Biochemistry 31*, 3862–3871.

(10) Danielson, M. A., and Falke, J. J. (1996) Use of F-19 NMR to probe protein structure and conformational changes. *Annu. Rev. Biophys. Biomol. Struct. 25*, 163–195.

(11) Salgado, J., Grage, S. L., Kondejewski, L. H., Hodges, R. S., McElhaney, R. N., and Ulrich, A. S. (2001) Membrane-bound structure and alignment of the antimicrobial β-sheet peptide Gramicidin S derived from angular and distance constraints by solid state F-19-NMR. *J. Biomol. NMR 21*, 191–208.

(12) Gerig, J. T. (1994) Fluorine NMR of Proteins. *Prog. Nucl. Magn. Reson. Spectrosc. 26*, 293–370.

(13) Padlan, E. A., Silverton, E. W., Sheriff, S., Cohen, G. H., Smithgill, S. J., and Davies, D. R. (1989) Structure of an Antibody Antigen Complex: Crystal Structure of the Hyhel-10 Fab-Lysozyme Complex. *Proc. Natl. Acad. Sci. U.S.A. 86*, 5938–5942.

(14) Tsumoto, K., Nakaoki, Y., Ueda, Y., Ogasahara, K., Yutani, K., Watanabe, K., and Kumagai, I. (1994) Effect of the Order of Antibody Variable Regions on the Expression of the Single-Chain Hyhel10 Fv Fragment in *Escherichia coli* and the Thermodynamic Analysis of Its Antigen-Binding Properties. *Biochem. Biophys. Res. Commun. 201*, 546–551.

(15) Pomes, R., Wilson, R. C., and Mccammon, J. A. (1995) Free-Energy Simulations of the Hyhel-10/Hel Antibody-Antigen Complex. *Protein Eng. 8*, 663–675.

(16) Tsumoto, K., Ogasahara, K., Ueda, Y., Watanabe, K., Yutani, K., and Kumagai, I. (1995) Role of Tyr Residues in the Contact Region of Antilysozyme Monoclonal-Antibody Hyhel10 for Antigen-Binding. *J. Biol. Chem. 270*, 18551–18557.

(17) Tsumoto, K., Ogasahara, K., Ueda, Y., Watanabe, K., Yutani, K., and Kumagai, I. (1996) Role of salt bridge formation in antigen-antibody interaction: Entropic contribution to the complex between hen egg white lysozyme and its monoclonal antibody HyHEL10. *J. Biol. Chem. 271*, 32612–32616.

(18) Wibbenmeyer, J. A., Wagner, R. A., Xavier, K. A., Smith-Gill, S. J., and Willson, R. C. (1997) Testing the structural basis of lysozyme recognition by antibody HyHEL-5. *FASEB J. 11*, A834–A834.

(19) Wibbenmeyer, J. A., Wagner, R. A., Uehara, C. S., Smith-Gill, S. J., Schuck, P., and Willson, R. C. (1998) Contributions of salt bridges to the interaction of anti-lysozyme monoclonal antibody HyHEL-5 with lysozyme. *Abstr. Pap. Am. Chem. Soc. 216*, U327.

(20) Taylor, M. G., Rajpal, A., and Kirsch, J. F. (1998) Kinetic epitope mapping of the chicken lysozyme·HyHEL-10 Fab complex: Delineation of docking trajectories. *Protein Sci. 7*, 1857–1867.

(21) Rajpal, A., Taylor, M. G., and Kirsch, J. F. (1998) Quantitative evaluation of the chicken lysozyme epitope in the HyHEL-10 Fab complex: Free energies and kinetics. *Protein Sci. 7*, 1868–1874.

(22) Sharp, K. A. (1998) Calculation of HyHel10-Lysozyme binding free energy changes: Effect of ten point mutations. *Proteins: Struct., Funct., Bioinf. 33*, 39–48.

(23) Kondo, H., Shiroishi, M., Matsushima, M., Tsumoto, K., and Kumagai, I. (1999) Crystal structure of anti-hen egg white lysozyme antibody (HyHEL-10) Fv-antigen complex: Local structural changes

in the protein antigen and water-mediated interactions of Fv-antigen and light chain-heavy chain interfaces. *J. Biol. Chem. 274*, 27623−27631.
(24) Pons, J., Rajpal, A., and Kirsch, J. F. (1999) Energetic analysis of an antigen/antibody interface: Alanine scanning mutagenesis and double mutant cycles on the HyHEL-10/lysozyme interaction. *Protein Sci. 8*, 958−968.
(25) Shiroishi, M., Yokota, A., Tsumoto, K., Kondo, H., Nishimiya, Y., Horii, K., Matsushima, M., Ogasahara, K., Yutani, K., and Kumagai, I. (2001) Structural evidence for entropic contribution of salt bridge formation to a protein antigen-antibody interaction: The case of hen lysozyme-HyHEL-10 Fv complex. *J. Biol. Chem. 276*, 23042−23050.
(26) Kirsch, J. F., Pons, J., and Stratton, J. R. (2002) How do two unrelated antibodies, HyHEL-10 and F9.13.7, recognize the same epitope of hen egg-white lysozyme? *Protein Sci. 11*, 2308−2315.
(27) Mohan, S., Sinha, N., and Smith-Gill, J. (2003) Modeling the binding sites of anti-hen egg white lysozyme antibodies HyHEL-8 and HyHEL-26: An insight into the molecular basis of antibody cross-reactivity and specificity. *Biophys. J. 85*, 3221−3236.
(28) Li, Y. L., Urrutia, M., Smith-Gill, S. J., and Mariuzza, R. A. (2003) Dissection of binding interactions in the complex between the anti-lysozyme antibody HyHEL-63 and its antigen. *Biochemistry 42*, 11−22.
(29) Kumagai, I., Nishimiya, Y., Kondo, H., and Tsumoto, K. (2003) Structural consequences of target epitope-directed functional alteration of an antibody: The case of anti-hen lysozyme antibody, HyHEL-10. *J. Biol. Chem. 278*, 24929−24936.
(30) Yokota, A., Tsumoto, K., Shiroishi, M., Kondo, H., and Kumagai, I. (2003) The role of hydrogen bonding via interfacial water molecules in antigen-antibody complexation: The HyHEL-10-HEL interaction. *J. Biol. Chem. 278*, 5410−5418.
(31) Nakanishi, T., Tsumoto, K., Yokota, A., Kondo, H., and Kumagai, I. (2008) Critical contribution of VH-VL interaction to reshaping of an antibody: The case of humanization of anti-lysozyme antibody, HyHEL-10. *Protein Sci. 17*, 261−270.
(32) Acchione, M., Lipschultz, C. A., DeSantis, M. E., Shanmuganathan, A., Li, M., Wlodawer, A., Tarasov, S., and Smith-Gill, S. J. (2009) Light chain somatic mutations change thermodynamics of binding and water coordination in the HyHEL-10 family of antibodies. *Mol. Immunol. 47*, 457−464.
(33) Li, Y. L., Li, H. M., Yang, F., Smith-Gill, S. J., and Mariuzza, R. A. (2003) X-ray snapshots of the maturation of an antibody response to a protein antigen. *Nat. Struct. Biol. 10*, 482−488.
(34) Lipschultz, C. A., Li, Y. L., and Smith-Gill, S. (2000) Experimental design for analysis of complex kinetics using surface plasmon resonance. *Methods 20*, 310−318.
(35) Kourentzi, K., Srinivasan, M., Smith-Gill, S. J., and Willson, R. C. (2008) Conformational flexibility and kinetic complexity in antibody-antigen interaction. *J. Mol. Recognit. 21*, 114−121.
(36) Li, Y. L., Li, H. M., Smith-Gill, S. J., and Mariuzza, R. A. (2000) Three-dimensional structures of the free and antigen-bound Fab from monoclonal antilysozyme antibody HyHEL-63. *Biochemistry 39*, 6296−6309.
(37) Waugh, D. S. (1996) Genetic tools for selective labeling of proteins with alpha-N-15-amino acids. *J. Biomol. NMR 8*, 184−192.
(38) Lipschultz, C. A., Li, Y., and Smith-Gill, S. (2000) Experimental design for analysis of complex kinetics using surface plasmon resonance. *Methods 20*, 310−318.
(39) Burmester, J., Spinelli, S., Pugliese, L., Krebber, A., Honegger, A., Jung, S., Schimmele, B., Cambillau, C., and Pluckthun, A. (2001) Selection, characterization and X-ray structure of anti-ampicillin single-chain Fv fragments from phage-displayed murine antibody libraries. *J. Mol. Biol. 309*, 671−685.
(40) Clark, K. R., and Walsh, S. T. R. (2009) Crystal structure of a 3B3 variant-A broadly neutralizing HIV-1 scFv antibody. *Protein Sci. 18*, 2429−2441.
(41) Laskowski, R. A., Macarthur, M. W., Moss, D. S., and Thornton, J. M. (1993) Procheck: A Program to Check the Stereochemical Quality of Protein Structures. *J. Appl. Crystallogr. 26*, 283−291.
(42) Jaskolski, M., Gilski, M., Dauter, Z., and Wlodawer, A. (2007) Numerology versus reality: A voice in a recent dispute. *Acta Crystallogr. D63*, 1282−1283.
(43) Wlodawer, A., Minor, W., Dauter, Z., and Jaskolski, M. (2008) Protein crystallography for non-crystallographers, or how to get the best (but not more) from published macromolecular structures. *FEBS J. 275*, 1−21.
(44) Cotten, M., Tian, C. L., Busath, D. D., Shirts, R. B., and Cross, T. A. (1999) Modulating dipoles for structure-function correlations in the Gramicidin A channel. *Biochemistry 38*, 9185−9197.
(45) Wong, C. Y., and Eftink, M. R. (1998) Incorporation of tryptophan analogues into staphylococcal nuclease, its V66W mutant, and Δ137−149 fragment: Spectroscopic studies. *Biochemistry 37*, 8938−8946.
(46) Carver, J. P., and Richards, R. E. (1972) General 2-Site Solution for Chemical Exchange Produced Dependence of T2 Upon Carr-Purcell Pulse Separation. *J. Magn. Reson. 6*, 89.
(47) Dubois, B. W., and Evers, A. S. (1992) F-19-Nmr Spin Spin Relaxation (T2) Method for Characterizing Volatile Anesthetic Binding to Proteins: Analysis of Isoflurane Binding to Serum Albumin. *Biochemistry 31*, 7069−7076.
(48) Luz, Z., and Meiboom, S. (1963) Nuclear Magnetic Resonance Study of Protolysis of Trimethylammonium Ion in Aqueous Solution: Order of Reaction with Respect to Solvent. *J. Chem. Phys. 39*, 366.
(49) Luz, Z., and Meiboom, S. (1963) Kinetics of Proton Exchange in Aqueous Solutions of Acetate Buffer. *J. Am. Chem. Soc. 85*, 3923.
(50) Allerhand, A., and Gutowsky, H. S. (1964) Spin-Echo Nmr Studies of Chemical Exchange. 1. Some General Aspects. *J. Chem. Phys. 41*, 2115.
(51) Gottwald, A., Creamer, L. K., Hubbard, P. L., and Callaghan, P. T. (2005) Diffusion, relaxation, and chemical exchange in casein gels: A nuclear magnetic resonance study. *J. Chem. Phys. 122*, 34506.
(52) Ahmed, A. H., Loh, A. P., Jane, D. E., and Oswald, R. E. (2007) Dynamics of the S1S2 glutamate binding domain of GluR2 measured using F-19 NMR spectroscopy. *J. Biol. Chem. 282*, 12773−12784.